

Electrocaloric cooler combining ceramic multi-layer capacitors and fluid

Daniele Sette, Alexis Asseman, Mathieu Gérard, Hervé Strozyk, Romain Faye, and Emmanuel Defay^a

Materials and Research Technology Department, Luxembourg Institute of Science and Technology, 41 Rue du Brill, L-4422 Belvaux, Luxembourg

(Received 13 May 2016; accepted 9 August 2016; published online 1 September 2016)

In this paper, an electrocaloric (EC) cooler prototype made of 150 ceramic-based Multi-Layer Capacitors (MLCs) has been detailed. This cooler involves a column of dielectric fluid where heat exchange with the MLCs takes place. The maximum variation of temperature in the fluid column due to the EC effect reaches 0.13 K whereas the heat exchanged during one stroke is 0.28 J. Although this prototype requires improvements with respect to heat exchange, the basic principle of creating a temperature gradient in a column of fluid has been validated. © 2016 Author(s). All article content, except where otherwise noted, is licensed under a Creative Commons Attribution (CC BY) license (<http://creativecommons.org/licenses/by/4.0/>). [<http://dx.doi.org/10.1063/1.4961954>]

Electrocaloric (EC) materials exhibit a transient variation of temperature ΔT when exposed to an external electric field. During the last decade, the discovery of large $\Delta T > 15$ K in both polymers and ceramic materials^{1,2} has considerably renewed the fundamental and applicative interests in this EC effect.³ Although the EC effect has been known for more than 80 years now, there are only few examples of EC-based cooling devices in the literature.³ Interestingly, all the studies regarding EC coolers have been published between 2012 and 2016^{4–8} except Sinyavsky's prototypes published in 1989 and 1992.^{9,10} Fig. 1 displays the different strategies developed on EC cooling prototypes so far. They can be based on purely solid state devices or need a fluid to carry heat. The active EC material can be based on polyvinylidene (PVDF) polymers or on ceramics. These ceramics can be in bulk form or inside Multi-Layer Capacitors (MLCs) in which EC layers are sandwiched between metallic electrodes.¹¹ MLCs exhibit an interesting structure because they combine all the characteristics required to improve the EC effect, namely, (1) the EC layers are thin enough to potentially exhibit the so-called giant EC effect,¹ (2) the metallic electrodes can conduct heat very efficiently thanks to thermal conductivity roughly one hundred times larger than in EC ceramic layers, and (3) the MLC itself is sufficiently big to demonstrate enough heat to be used in a prototype, contrary to thin films. Moreover, MLCs are extremely reliable as they have been initially developed to act as large values capacitors and are currently used in plenty of electronic devices. Their main drawback—which will be hopefully only temporary—is that they do not rely on the best EC materials, as they have not been optimized for such kind of application. This problem should be overcome in the coming years as several teams skilled in the art are currently trying to optimize EC MLCs.^{12,13} They have nevertheless been already operated in two prototypes in Refs. 4 and 5 but in both cases, no fluid has been utilized to carry heat, contrary to the best EC prototype in terms of ΔT .¹⁰ In this study, we propose for the first time to combine MLCs with a dielectric fluid.

In our prototype, sketched in Fig. 2, heat exchange takes place between a column of dielectric fluid¹⁴ and EC plates made of commercially available Zr-doped BaTiO₃ (Zr-BTO) MLCs.¹⁵ The dimensions of each MLC are $3.2 \times 2.5 \times 2$ mm³. Polishing one of these MLCs enabled us to observe that they are made of 183 layers of 10 μ m-thick Zr-BTO sandwiched between

Note: Invited for the Caloric Materials special topic.

^aAuthor to whom correspondence should be addressed. Electronic mail: emmanuel.defay@list.lu

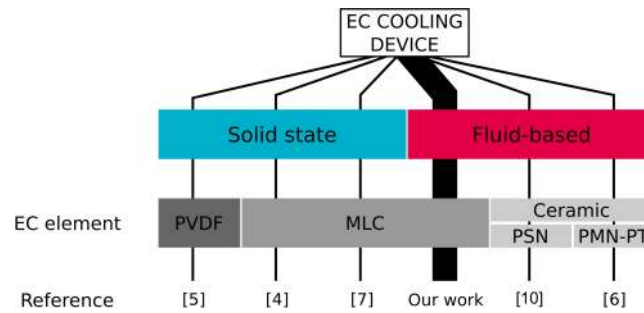


FIG. 1. Strategy developed in the literature regarding EC prototypes with different EC materials (polymers or ceramics) and different ways of carrying heat (solid-state or fluid).

184 $2 \mu\text{m}$ -thick interdigitated electrodes made of Ni. These electrodes are alternatively connected to one of the two electrical terminals, made of an alloy based on tin. As depicted in the inset of Fig. 2, three EC plates are assembled altogether. During cycling, they are displaced up and down in the column of fluid. The travel distance is 80 mm. Each of these plates is made of 50 MLCs connected in parallel between two copper foils. Silver-loaded epoxy has been used to glue the MLCs with the copper foils. Note in the inset of Fig. 2 that the MLCs are connected through their terminals, which infers that contact between fluid and MLCs plates is mostly performed through the terminals. The orientation of the Ni-electrodes is perpendicular to the terminals that collect heat generated into the MLCs by the EC effect and eventually exchange heat with the fluid. The three plates are connected in parallel with $100 \mu\text{m}$ -diameter copper leads, which allows for applying voltage to trigger the EC effect. The application of voltage is synchronized with the plates' position thanks to a pneumatic piston, as shown in Fig. 2. Temperature is monitored through cycling thanks to three 1/3 DIN Pt100 thermometers—two at the extremities of the column of fluid and one on the central MLCs plates.

As detailed in Fig. 3(a), the applied thermodynamic cycle is based on a modified Brayton cycle with six steps. It involves two adiabatic legs (from step 2 to 3 and 5 to 6), two iso-field legs with plates in stationary position (from step 3 to 4 and 6 to 1), and two iso-field legs during plate moves (from step 4 to 5 and 1 to 2). The ideal working principle of this cycle is depicted in Fig. 3(b), in which the outer and inner rectangles stand respectively for the column of fluid and the EC plates. In step 1, EC plates are at the lowest position and they are ideally at the same temperature (cold) as the fluid. The plates are then lifted up with the piston, exchanging some heat with the fluid. When they reach the highest position, the plates are in step 2. Then voltage is applied ($V = V_0$) heating up the plates because the MLCs exhibit a positive EC effect. It is step 3. From step 3 to 4, heat is

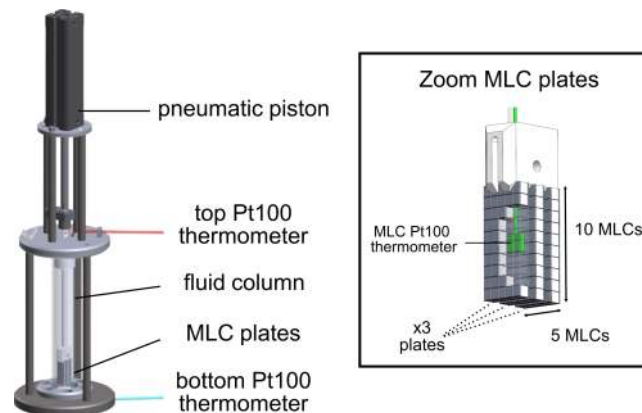


FIG. 2. Experimental setup involving 150 MLCs assembled in three plates of 50 MLCs each immersed in a column of dielectric fluid. A piston is used to displace the EC plates up and down in a synchronized way with respect to the voltage application that triggers the EC effect in the plates. Temperature is monitored by Pt100 thermometers at the top (T_{top}) and bottom (T_{bottom}) locations of the fluid column and also on the middle MLCs plate (cf. inset).

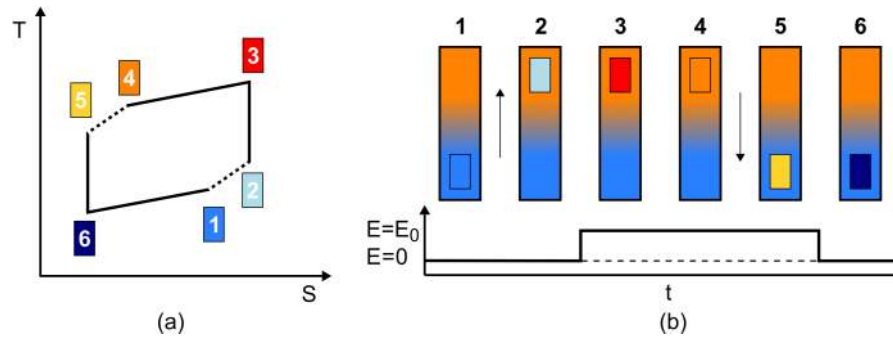


FIG. 3. (a) Modified-Brayton thermodynamic cycle used in this study. There are two adiabatic legs (2-3 and 5-6), two iso-field legs with plates in stationary position (3-4 and 6-1), and two iso-field legs during plate moves (4-5 and 1-2). (b) State of the fluid column (large outer rectangles) and the EC plates (smaller inner rectangles) during the six steps of the modified-Brayton cycle. The step numbers fit with the ones displayed in (a). The different colours in the two schemes represent the temperature during cycling in an intuitive manner (the bluer the colder, the redder the hotter).

exchanged between the plates and the fluid in a static position. Voltage is still on. After some time, ideally when $T_{\text{plates}} = T_{\text{fluid}}$, the plates start to be pulled down (step 4), always with voltage on. They reach the lowest position at step 5, with voltage on. Then, voltage is released at step 5 ($V = 0$), which induces cooling down the EC plates. This in turn cools down the fluid between step 6 and step 1.

According to the manufacturer, the absolute temperature precision obtained with 1/3 DIN thermocouples is ± 0.10 K, which is not accurate enough to extract a reliable absolute temperature in our case. However, we observed that the reproducibility of the variations of temperature measured in our experiment is around 1 mK, which corresponds to the electronic amplification resolution (PT-104 data logger from Picotech). This is why we will only report relative variations of temperatures in this paper. Note that we have checked that the variation of temperature of the MLC plates in air when supplied at 200 V is identical when measured by IR camera, according to the technique detailed in Ref. 16. The three plates are connected to one single Keithley 2400 source meter. The prototype has been covered with several layers of thermal insulator in order to avoid thermal disturbances from the surroundings. Piston travelling time is constant and has been set at 2 s. The maximum voltage applied to the MLCs is 200 V, supplied at 30 mA-constant current. Note that it takes 1.3 s to charge the 150 capacitors in these conditions.

Fig. 4(a) shows the temperature differences measured at the top (red) δT_{top} and bottom (blue) δT_{bot} of the column of fluid during cycling. The reference temperature is the one at t_0 . As already mentioned, we display temperature differences instead of absolute temperatures in order to improve accuracy but also to artificially suppress the remanent temperature in the fluid column induced by the movement of the piston when no voltage is applied to the plates. Using temperature difference gives the opportunity to only consider the electrocaloric effect. However, let us mention that the overall range of absolute temperatures in these experiments—taking into account the EC effect, the piston heating, and the variation of ambient temperature—remains between 24 and 24.9 °C. For such small variation of temperature, Kar Narayan *et al.* have shown that the EC effect of similar MLCs exhibits very little variation, as depicted in Fig. 2(d) of Ref. 17. Thanks to this figure, the estimation in our case is a variation of the EC effect of less than 3% between 24 and 24.9 °C, which is negligible.

In Fig. 4(a), the duration of the two iso-field static legs is 18 s and the transition duration from top to bottom of the column and the other way round is 2 s, which means that a cycle lasts for 40 s. In Figs. 4(a) and 4(b), the voltage application on the EC plates starts at $t_0 = 0$ s according to the cycle description given in Fig. 3. Note that the piston was moving several hours before t_0 . A first sequence from t_0 to $t = 600$ s shows a clear increase of δT_{top} and decrease of δT_{bot} . A second sequence from $t = 600$ s to $t = 2700$ s shows that δT_{top} and δT_{bot} remain roughly constant. The difference between δT_{top} and δT_{bot} , labelled $\Delta(\delta T)$, is displayed in Fig. 4(b) and shows that the temperature difference between the top and the bottom of the fluid column due to the EC

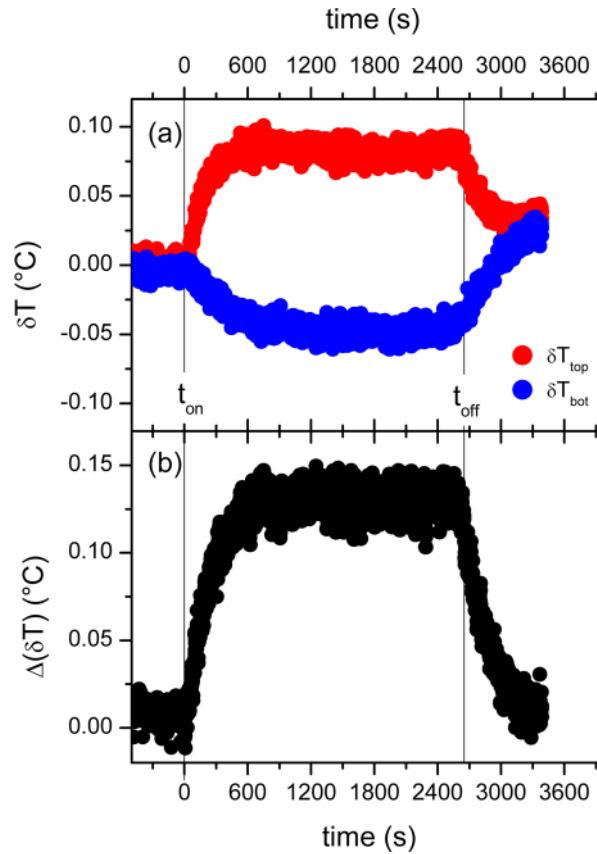


FIG. 4. (a) Temperature difference δT versus time of the top (δT_{top}) and the bottom (δT_{bot}) temperature of the column of fluid while cycling. The reference temperature is the one at t_0 . and (b) difference between δT_{top} and δT_{bot} , labelled $\Delta(\delta T)$. These temperature differences were displayed instead of temperature to suppress the remanent temperature induced by the movement of the EC plates when no voltage was applied. For both figures, voltage on MLCs was applied according to the cycle detailed in Fig. 3 between $t = 0$ s and $t = 2700$ s. The plates were moved according to a 40 s-period cycle during the whole experiment.

effect is constant during this second sequence, reaching the maximum value of 0.13 K. The voltage application is stopped after 2700 s, though the piston still moves the plates up and down. This stop immediately induces the decrease of δT_{top} and the increase of δT_{bot} , as a direct consequence of the cancellation of the EC effect on the MLC plates. δT_{top} and δT_{bot} join at $\delta T = 0.03$ K after 3300 s as a consequence of the piston heating.

Fig. 5 displays the variation of temperature ΔT_{plate} measured on the central MLC plate during the first four cycles. The number of each step of the cycle described in Fig. 3(a) has been reported in these four cycles. In Fig. 5, one can immediately spot the 40 s-period of one cycle. The first temperature jump induced by the applied voltage happens when the plates are in the highest position. It is therefore an adiabatic variation of temperature nearly corresponding to the leg from step 2 to 3, as depicted in Fig. 3(b). However, the difference is that the initial temperatures of the plates and the fluid are identical, contrary to what will happen in the subsequent cycles (cf. Fig. 3(b) at steps 2 and 3). Therefore, this first temperature jump allows for identifying the intrinsic EC adiabatic ΔT_{plate} in fluid, which is 0.54 K. The plates then remain in up position for 18 s with voltage on, letting heat being transferred from the plates to the fluid (3 to 4). Interestingly, the maximum ΔT_{plate} occurs after 5-7 s after the initial jump. The rather low thermal conductivity of the fluid, which is approximately 10 times lower than water, infers a slow thermal transfer from the plates to the fluid. Consequently it takes time to heat up or cool down the fluid when the plates' temperature change occurs. As the Pt100 thermometer is at the interface between the plate and the fluid, it seems plausible that there is a delay before it reaches its optimum temperature. At the end of step 4, the plates are moved to the

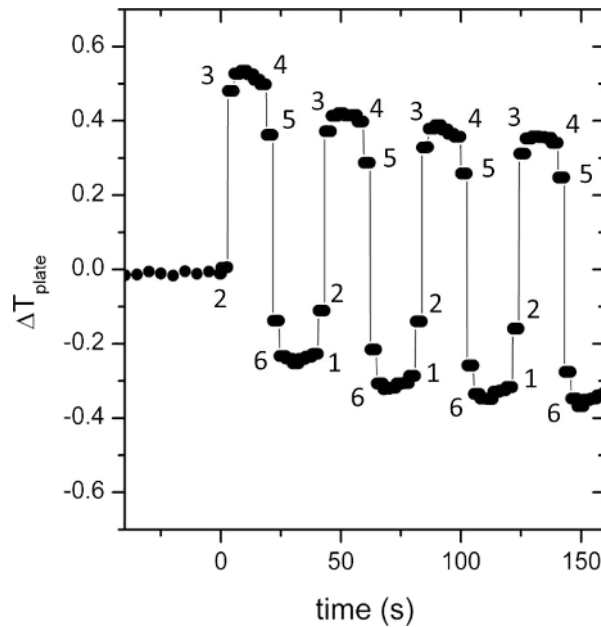


FIG. 5. Variation of temperature ΔT_{plate} measured on the central MLC plate during the first four Brayton cycles depicted in Fig. 3.

lowest position still at voltage on, reaching step 5 in Fig. 5. The variation of temperature induced by this iso-field leg is difficult to extract from our data set as there is only one measurement point every 2.7 s (it also means that the position of points 5 in Fig. 5 is only an indication). If one considers that the amplitude of the positive and negative adiabatic ΔT_{plate} is identical—0.54 K—then we can deduce that the temperature jump at step 6 goes from -0.18 K for the first cycle to -0.13 K for the fourth cycle. At step 6, voltage is removed, which triggered the cooling EC effect. ΔT_{plate} of steps 5 and 6 reaches -0.72 K for this first cycle. From step 6 to step 1, heat is transferred from the static plates to the fluid. After 18 s, step 1 is reached and the plates are put back to the upper position in 2 s, with no voltage applied. It is step 2, where a temperature jump similar (but positive) to the one of step 6 occurs ($+0.05$ K). Note that the amplitude of this temperature jump is larger at step 6 than at step 3, for the first cycles. This is the reason why ΔT_{plate} becomes little by little symmetrical with time with respect to $\Delta T_{\text{plate}} = 0$ K. Indeed, the temperature jumps occurring during these two iso-field steps are proportional to the difference between the temperature of the plates and the temperature of the fluid. At the beginning, this difference is larger for negative steps. But after some cycles, it tends to become identical, which stabilizes the temperature pattern with time (after 8-9 cycles, not represented in Fig. 5).

Besides, we assessed the role played by the piston on this prototype. When the cycle period is respectively 10, 20, and 40 s and no EC effect is activated, the temperature difference between the top and the bottom of the fluid column is respectively 0.23, 0.18 K, and 0.13 K. Therefore, the shorter the period, the larger the piston influence on the prototype temperature. It emphasizes the negative role played by the piston. It is clear that next generations of prototypes should not involve a piston with the fluid.

The maximum variation of temperature in the column of fluid of 0.13 K is rather low compared with the literature, where it goes from 0.3 K in Ref. 4 to 5 K in Ref. 10. The main reason is the poor heat exchange between the MLCs and the fluid. Indeed, in this simple prototype, this exchange takes place only during static positions of the plates and only a small fraction of heat goes out from the plates by heat conduction. One can estimate the heat exchanged per stroke from $\Delta T_{\text{plate}} \sim 0.05$ K occurring during the iso-field legs, as extracted from Fig. 5, even though we observed that the fluid disturbs the measurement of the real temperature change. The mass of one MLC is 0.087 g. As it is made of Ni and BTO both exhibiting a specific heat around $430 \text{ J K}^{-1} \text{ kg}^{-1}$ (Ref. 11), the MLCs heat capacity is 37 mJ K^{-1} . Therefore the heat induced by 150 MLCs for one stroke reaches 0.28 J. This

value could be as large as 4.8 J by implementing a proper heat exchange—for instance, based on forced convection as performed in Ref. 10—that would collect all the heat generated by the MLCs. This value would then be comparable with what is still considered as the best EC fridge ever.¹⁰ Note that the cycling frequency of our prototype is only 25 mHz whereas it can reach values as high as 4 Hz in Ref. 10. This cycling frequency is the optimal case for $\Delta(\delta T)$ (cf. Fig. 4(b)) in our prototype, the reason being again the poor heat exchange imposing to stay for a long time during each iso-field leg.

Although this analysis shows this prototype requires improvements with respect to heat exchange, the basic principle of creating a temperature gradient in a column of fluid has been validated with commercially available MLCs. Two main modifications will be performed in our future prototype: (1) no direct interaction of the piston with the fluid, to avoid friction and (2) heat exchange will be performed via convection of fluid and plates instead of conduction by strongly decreasing the fluid column section.

The authors thank N. D. Mathur and X. Moya for valuable discussions. This work was entirely supported by the Fonds National de la Recherche (FNR) of Luxembourg through the project CO-FERMAT belonging to the PEARL scheme.

- ¹ A. S. Mischenko, Q. Zhang, J. F. Scott, R. W. Whatmore, and N. D. Mathur, *Science* **311**, 1270–1271 (2006).
- ² B. Neese, B. Chu, S.-G. Lu, Y. Wang, E. Furman, and Q. M. Zhang, *Science* **321**, 821–823 (2008).
- ³ X. Moya, S. Kar-Narayan, and N. D. Mathur, *Nat. Mater.* **13**, 439 (2014).
- ⁴ Y. Jia and S. Ju, *Appl. Phys. Lett.* **100**, 242901 (2012).
- ⁵ H. Gu, X. Qian, X. Li, B. Craven, W. Zhu, A. Cheng, S. C. Yao, and Q. M. Zhang, *Appl. Phys. Lett.* **102**, 122904 (2013).
- ⁶ U. Plaznik, A. Kitanovski, B. Rožič, B. Malič, H. Uršič, S. Drnovšek, J. Cilenšek, M. Vrabelj, A. Poredoš, and Z. Kutnjak, *Appl. Phys. Lett.* **106**, 043903 (2015).
- ⁷ Y. D. Wang, S. J. Smullin, M. J. Sheridan, Q. Wang, C. Eldershaw, and D. E. Schwartz, *Appl. Phys. Lett.* **107**, 134103 (2015).
- ⁸ P. Blumenthal, C. Molin, S. Gebhardt, and A. Raatz, *Ferroelectrics* **497**(1), 1–8 (2016).
- ⁹ Y. V. Sinyavsky, N. D. Pashkov, Y. M. Gorovoy, and G. E. Lugansky, *Ferroelectrics* **90**, 213 (1989).
- ¹⁰ Yu. Sinyavsky and V. M. Brodyansky, *Ferroelectrics* **131**, 321 (1992).
- ¹¹ S. Kar-Narayan and N. D. Mathur, *Appl. Phys. Lett.* **95**, 242903 (2009).
- ¹² S. Crossley, T. Usui, B. Nair, S. Kar-Narayan, X. Moya, S. Hirose, A. Ando, and N. D. Mathur, *Appl. Phys. Lett.* **108**, 032902 (2016).
- ¹³ H.-J. Ye, X.-S. Qian, D.-Y. Jeong, S. Zhang, Y. Zhou, W.-Z. Shao, L. Zhen, and Q. M. Zhang, *Appl. Phys. Lett.* **105**, 152908 (2014).
- ¹⁴ WACKER AK100 Silicone Fluid.
- ¹⁵ MULTICOMP MC1210F476Z6R3CT.
- ¹⁶ S. Kar-Narayan, S. Crossley, X. Moya, V. Kovacova, J. Abergel, A. Bontempi, N. Baier, E. Defay, and N. D. Mathur, *Appl. Phys. Lett.* **102**, 032903 (2013).
- ¹⁷ S. Kar-Narayan and N. D. Mathur, *J. Phys. D: Appl. Phys.* **43**, 032002 (2010).